

Supporting Information

Stott et al. 10.1073/pnas.1012539107

SI Text

SI Materials and Methods. HB-Chip device fabrication. Negative photoresist (SU-8, MicroChem, Newton, MA, USA) was photolithographically patterned on silicon wafers to create masters with two-layer features. The first SU-8 features form the main microfluidic channel and the second layers form the herringbone structures. The heights of SU-8 features (ranging from 25–75 μm) on the masters were measured with a surface profilometer (Dektak ST System Profilometer, Veeco Instruments Inc., Plainview NY). The masters were then used as molds, on which polydimethylsiloxane (PDMS) prepolymer mixed with its crosslinker at 10:1 weight ration was poured, degassed, and allowed to cure in a conventional oven at 65 $^{\circ}\text{C}$ for 24 h. The cured PDMS replicas were removed from the molds, subjected to a brief oxygen plasma treatment, and bonded to glass substrates to form the final devices.

To chemically modify the device, the microfluidic channels were treated with 4% (v/v) solution of 3-mercaptopropyl trimethoxysilane (Gelest, Morrisville, PA) in ethanol for 1 h at room temperature, followed by incubation in 0.01 $\mu\text{mol mL}^{-1}$ N-y-maleimidobutyryloxy succinimide ester (GMBS) (Pierce Biotechnology, Rockford, IL) in ethanol for 30 min at room temperature. Next, the channels were filled with 10 $\mu\text{g mL}^{-1}$ NeutrAvidin (Pierce Biotechnology, Rockford, IL) solution in PBS for 1 h to attach NeutrAvidin to the GMBS. Devices were stored in avidin at 4 $^{\circ}\text{C}$ until use. Within 24 h of the experiment, 20 $\mu\text{g/mL}$ biotinylated goat antihuman EpCAM (R and D Systems, Minneapolis, MN) solution in PBS containing 1% (w/v) bovine serum albumin (BSA) (Sigma Aldrich, St. Louis, MO) and 0.09% (w/v) sodium azide were added to the devices. Ethanol or PBS was used to rinse unbonded molecules after each reaction, depending on the solvent used in the previous step. For coating IgG antibody, biotinylated normal goat IgG (R and D Systems, Minneapolis, MN) was in place of the biotinylated EpCAM. One hour prior to running the HB-Chip, devices were purged with 3% BSA with 0.05% Tween20 (Fisher Scientific, Pittsburgh, PA).

Hematoxylin and eosin staining. Following immunofluorescence staining, a subpopulation of devices was selected for subsequent staining with a hematoxylin and eosin protocol customized for the flow-through conditions required by the chip. Devices previously stored in saline solution at 4 $^{\circ}\text{C}$ postIF staining were flushed with deionized water using a syringe pump. Thinprep nuclear stain (Cytoc Corp., Marlborough, MA), was applied under flow, and followed by a wash with deionized water. Next, Shandon bluing reagent (Thermo Scientific, Waltham, MA) was added, followed by a deionized water rinse. Finally, 1% aqueous eosin stain (Sigma Aldrich, St. Louis, MO) was added, and the device was washed and stored in deionized water. Chips are imaged under bright field illumination within 24 h of staining.

RT-PCR analysis and sequencing. Circulating tumor cell RNA was isolated from devices by infusion of TRIzol Reagent (Invitrogen, Carlsbad, CA) and incubation at room temperature, followed by elution of cell lysate. Total RNA was extracted from the eluted lysate according to the manufacturer's protocol. First-strand cDNA synthesis was performed using the Superscript III First-Strand Synthesis System for RT-PCR (Invitrogen) following manufacturer instructions. The TMPRSS2-ERG fusion was PCR-amplified using Fidelitaq PCR Master Mix (USB, Cleveland, OH) and the following nested primer pairs: Primary PCR primers, TMPRSS2.F: 5'CGCCTCCTGAGATTAAAGC-

GAGAGC-3' and ERG.R: 5'-GCCTCTGGAAGTCGTC-CTTG-3'; secondary PCR primers, TMPRSS2.SECF: 5'-CAG-GAGGCGGAGGCGGA-3' and ERG.SECR: 5'-GGAATAACAAGATCTTGACGTCTGG-3'. PCR amplicons were purified using exonuclease I and shrimp alkaline phosphatase (United States Biochemical, Cleveland, OH), and termination based fluorescent sequencing was performed using the ABI BigDye Terminator kit v1.1 (ABI, Foster City, CA) and an ABI 3100 genetic analyzer. Sequencing electropherograms were compared to the reference sequences for TMPRSS2 and ERG (NM_005656.3 and NM_004449.4, respectively) to determine translocation events.

On-chip fluorescence in situ hybridization (FISH). Interphase FISH on cells captured on the device was performed according to standard protocols, with the following modifications. Briefly, after fixation of cells with paraformaldehyde, the device was infused with Digest-All 3 Pepsin solution (Invitrogen) and incubated at 37 $^{\circ}\text{C}$ for 10 min. The device was then washed by infusion of 2X SSC, dehydrated in an ascending series of alcohol, and air-dried. AR/CEP-X probe mix (Vysis LSI Androgen Receptor Xq12 SpectrumOrange Probe; Vysis CEP X DXZ1 Spectrum-Green Probe; Abbott Molecular, Des Plaines, IL) was infused, and the device was sealed with rubber cement. DNA was denatured at 75 $^{\circ}\text{C}$ for 5 min and hybridized at 37 $^{\circ}\text{C}$ for 20 h in a humidified hybridization oven. Posthybridization washes were performed in 0.4X SSC/0.3% NP-40 at 72 $^{\circ}\text{C}$, 2X SSC/0.1% NP-40 at room temperature, and then 2X SSC. Nuclei were counterstained with DAPI. The device was sealed with rubber cement and viewed by fluorescence microscopy.

Device imaging. HB-Chips were scanned on an automated upright fluorescence microscope (Eclipse 90i, Nikon, Melville, NY) under 10X magnification, in three z-planes. Three different emission spectra (DAPI, fluorescein isothiocyanate, and Texas Red) were captured using predetermined exposure times. After acquisition, images (~9,000 per chip) were analyzed using an algorithm developed in LabView 8.5 with IMAQ 3.5 (S1). The cells that were isolated as potential CTC targets were then evaluated by a human reviewer in a blinded fashion. The three-dimension projection of the prostate CTC cluster (Movie S5) was obtained by taking image slices in 1 μm increments using a confocal microscope (A1R-A1, Nikon, Melville, NY).

Microfluidic flow visualization experiments. A variation on our traditional small footprint herringbone microfluidic device was used for all flow visualization experiments, in which two separate streams join together at the chamber inlet (see Fig. S1 A, B). The fluid used in the mixing experiments was a mixture of glycerol and water (80/20), with 50 nm fluorescently labeled latex particles (Duke Scientific, Palo Alto, CA) added to one mixture to allow for observation of the two streams interacting. The resulting kinematic viscosity for the solution was 99.17 cSt, and the dynamic/absolute viscosity was 119.88 cP. For the solutions created to match the viscosity of whole blood, the kinematic viscosity was 3.31 cSt, and the dynamic/absolute viscosity was 3.5 cP. The Refutas equation was used to obtain the correct ratio of glycerol and water for all solutions. A syringe pump (PHD 22/2,000 Syringe Pump, Harvard Apparatus, Holliston, MA) was used to drive both flow streams through the device. For multiplane imaging of the flow inside the device, the images were acquired on a confocal microscope (LM510, Zeiss, Peabody, MA) at 0.7 μm increments.

To illustrate the flow along the entire footprint of the device, a series of stitched images were obtained using an inverted fluorescent microscope with an automated stage (Eclipse TiE, Nikon, Melville, NY).

Cell line preparation. Two cancer cell lines, NCI-H1650 and PC3 (ATCC, Manassas, VA), were cultured at 37 °C in 5% CO₂ in RPMI-1640 (H1650s) or F-12K (PC3s) growth medium containing 1.5 mM L-glutamine supplemented with 10% FBS and 1% Penicillin/Streptomycin with media changes every 2–3 d. Prior to spiking into whole blood, all cells were prelabeled with a fluorescent cellular dye (CellTracker™ Red, Invitrogen, Carlsbad, CA) following the manufacturers' recommended protocol. Cells were released through incubation in 0.05% Trysin-0.53 mM EDTA (Invitrogen, Carlsbad, CA) at 37 °C for 5–7 min, and a protein buffer was added to quench the protease activity. The cell titre was determined by an average of two measurements with a Coulter Counter (Beckman Coulter, Fullerton, CA), and the suspension was subsequently serially diluted to the desired concentration. Experiments were performed using H1650 and PC3 cells suspended in serum-free medium or spiked into healthy donor whole blood.

Microfluidic cancer cell line experiments. Spiked cell experiments were performed with either the small scale HB-Chip (one channel wide) with the waste capture device serially attached (Fig. S4), or the large scale HB-Chip (Fig. 1A). Experiments with the large scale HB-Chip were processed with the standard CTC processing machine (S2), utilizing the same processing conditions as the cancer patient samples. Large HB-Chips were subsequently imaged and enumerated using our automated image processing system

(S1). All device preparations and processing conditions for the CTC-Chip were run as previously described (S2). For experiments with the small scale HB-Chip, all spiked cell samples were preloaded into a 1 mL syringe and flowed through the device using a syringe pump (PHD 22/2,000 Syringe Pump, Harvard Apparatus). To keep cells from settling in the syringes, a small magnetic stir bar (Fisher Scientific, Pittsburgh, PA) was loaded into each syringe and a magnet was used to gently mix the blood periodically (~10 min intervals). The waste collection device was connected serially to the capture chamber, and was preloaded with 4% Para formaldehyde and Hoechst dye. The volumes entered into the small HB-Chip were selected such that the waste collection device would contain all spiked blood and subsequent rinse buffers that followed capture. After the rinse steps were completed, the waste collection device was removed and cells captured in the microchannels were fixed with 4% paraformaldehyde (Electron Microscopy Sciences, Hatfield, PA) in PBS solution, followed by Hoechst (Sigma Aldrich, St. Louis, MO) in 0.2% Triton-X 100 (Sigma Aldrich, St. Louis, MO) in PBS. Finally, the channels were rinsed with PBS solution. Both the microfluidic capture device and waste chamber were counted by hand on a fluorescence microscope. Capture efficiency was calculated as the number of spiked cells captured in the HB-Chip divided by the total number of cells flowed through the device (i.e., the number of cells captured plus the number of cells in waste collection device). For the full-scale HB-Chip experiments, capture efficiency was calculated as number of target cells captured divided by the total number of target cells that were sent through the device (based on cancer cell-spiking concentrations). Sample purity was defined as the number of target cells captured divided by the total number of nucleated cells bound to the device.

1. Stott, SL (2010) Isolation and characterization of circulating tumor cells from patients with localized and metastatic prostate cancer. *Sci Transl Med* 2:25ra23

2. Nagrath S (2007) Isolation of rare circulating tumor cells in cancer patients by microchip technology. *Nature* 450:1235–1239.

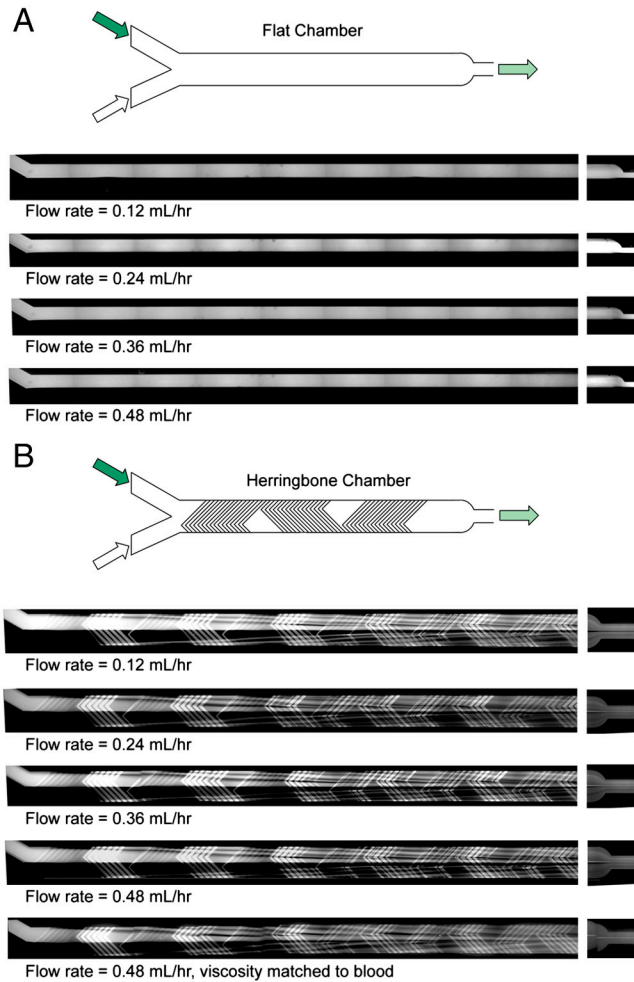


Fig. 51. Flow profiles to illustrate the differences in fluid mixing between a traditional smooth walled chamber (A) and the HB-Chip (B) at variable flow rates. For both devices, two fluid streams of matched viscosity (99.17 cSt) are input into the device, with one stream fluorescently labeled to highlight the interactions between the two streams as they travel through the length of the device. (A) Stitched fluorescent micrographs of the flat chamber device demonstrate the complete lack of interaction between the two input streams for the entire device at all flow rates explored. Due to size limitations, only the first 25% of the device is shown, with the exit of the device shown after the image break. For the herringbone chamber (B), the corresponding micrographs show that mixing of the two streams initiates immediately for all flow rates, with full mixing achieved within 20 mm of travel. As the viscosity of the two solutions is decreased to match that of whole blood (B, final frame, kinematic viscosity = 3.31 cSt), it can be seen that complete mixing of the two solutions initiates more rapidly. See *Results* and *SI Materials and Methods* for more details.

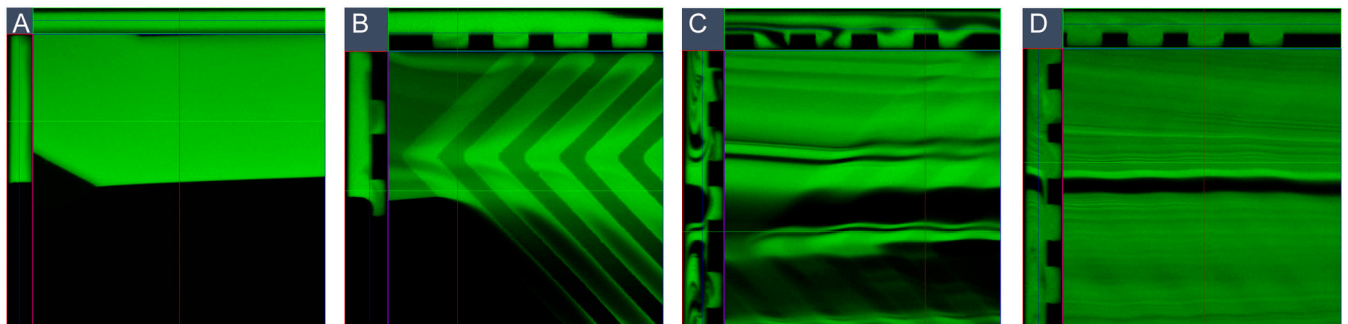


Fig. 52. Orthogonal projections of the fluid flow profiles for (A) the inlet of the flat chamber device, (B) the inlet of the herringbone device, (C) after one cycle of herringbone grooves, and (D) at the exit of the herringbone device. Micrographs are extracted from image stacks taken on a confocal microscope in $0.7\ \mu\text{m}$ intervals along the z-axis. Corresponding videos illustrating the flow profiles at all heights can be seen in *Movie S1*, *Movie S2*, *Movie S3*, and *Movie S4*.

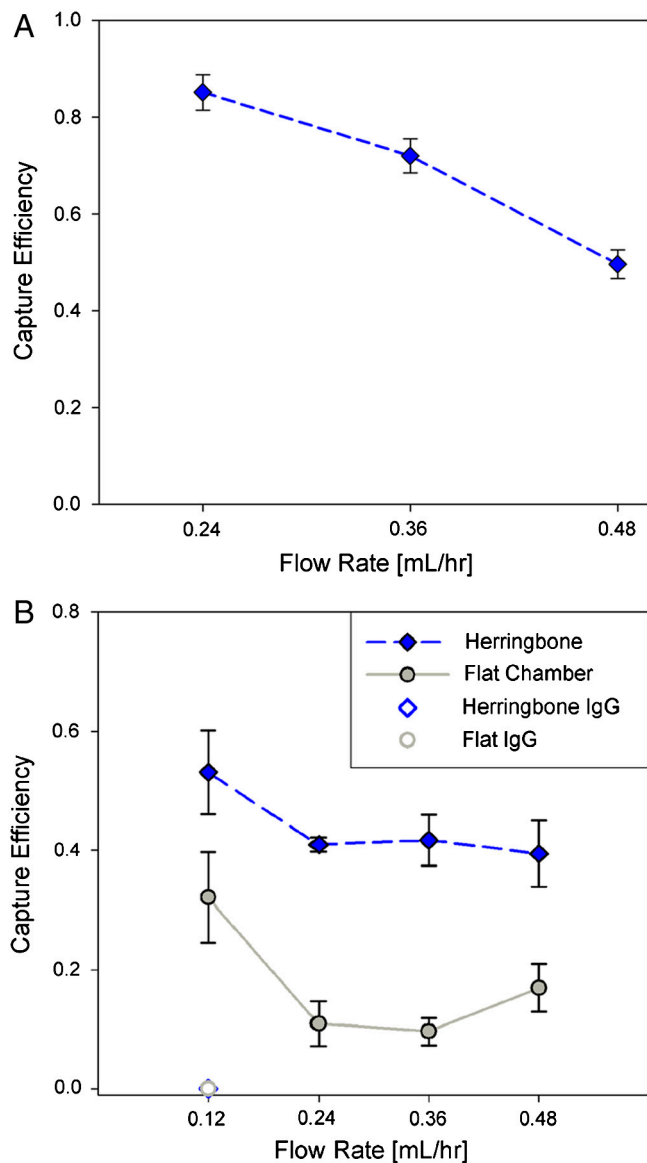


Fig. S3. (A) Additional proof-of-principle studies with a high EpCAM expressing cell line, H1650 cells (lung, >500,000 EpCAM molecules per cell) spiked into buffer at 5,000 cells/mL and processed at variable flow rates with the small version HB-Chip (true mass balance efficiency). Data was generated for comparison with data presented previous for the CTC-Chip (S2) which demonstrated a marked decline in capture efficiency as flow rate was increased. Note, the flow rates presented here are scaled by a factor of 10 to account for the changes in device scale. (B) Capture efficiency data for H1650 cells spiked into whole blood at 5,000 cells/mL and processed on the HB-Chip and a traditional flat-walled microfluidic device at variable flow rates. Nonspecific IgG capture antibody controls are also shown.

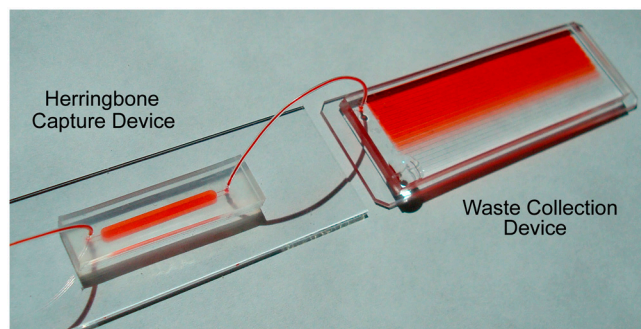


Fig. S4. Photograph of the small footprint herringbone capture device with the microfluidic waste collection device serially connected. The herringbone capture device consists of one herringbone channel (or 1/10th of the large scale HB-Chip size) and initial geometric parameters (channel height set to 70 μm , groove height set to 30 μm). The final, full sized HB-Chip was optimized to a channel height set to 50 μm , groove height set to 40 μm . Due to the differences in scale, all flow rates for the small herringbone device must be decreased by a factor of 10 from that of the full size HB-Chip. The microfluidic waste collection device was designed to have a serpentine pattern, allowing full collection of all fluids that travel through the capture device. The height of the waste chamber (50 μm) was selected so that fluorescently labeled spiked cells can still be viewed through whole blood. This microfluidic device setup enables a true mass balance for capture efficiency calculations, removing any errors from cell-spiking inaccuracies.

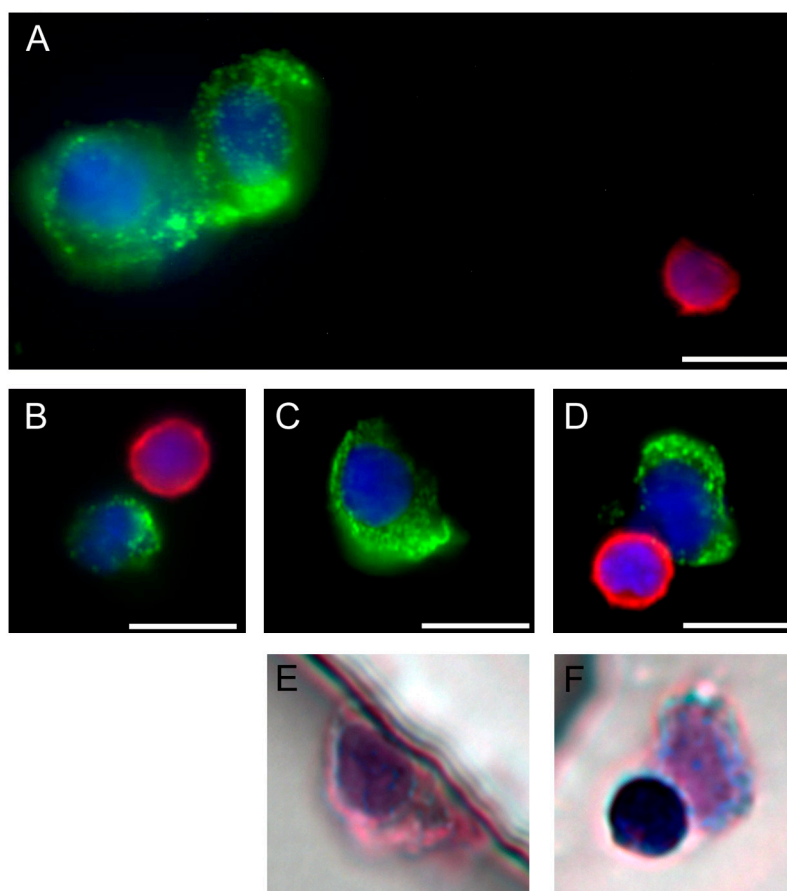
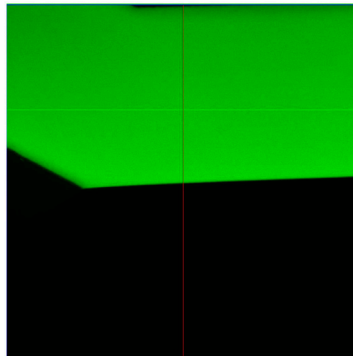
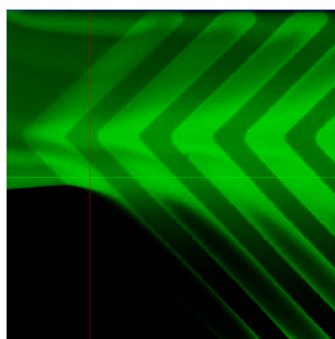


Fig. S5. Micrographs of CTCs isolated from a single metastatic lung cancer patient, demonstrating the heterogeneity in captured cell size (A–D). Captured cells were fluorescently stained for cytokeratin 7/8 (green), CD45 (red), and DNA (blue). Corresponding H and E images (E–F) are provided for cells shown in (C–D). (Scale bar: 10 μm).



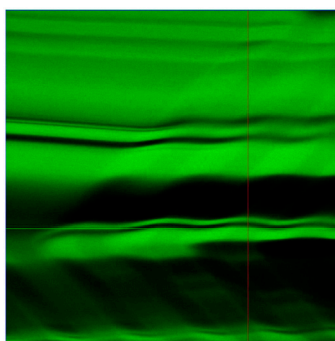
Movie S1. Videos generated from image stacks taken on a confocal microscope in 0.7 μm intervals along the z-axis of the devices shown in Fig. S1. Movie S1 depicts the flow profile for the inlet of the flat chamber device.

[Movie S1 \(MPG\)](#)



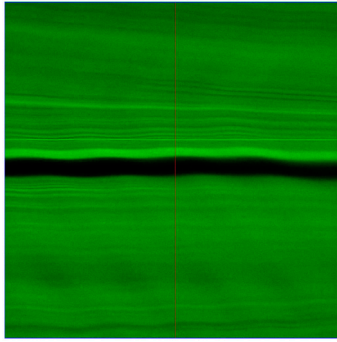
Movie S2. Movie S2 illustrates the profiles at the inlet of the herringbone device.

[Movie S2 \(MPG\)](#)



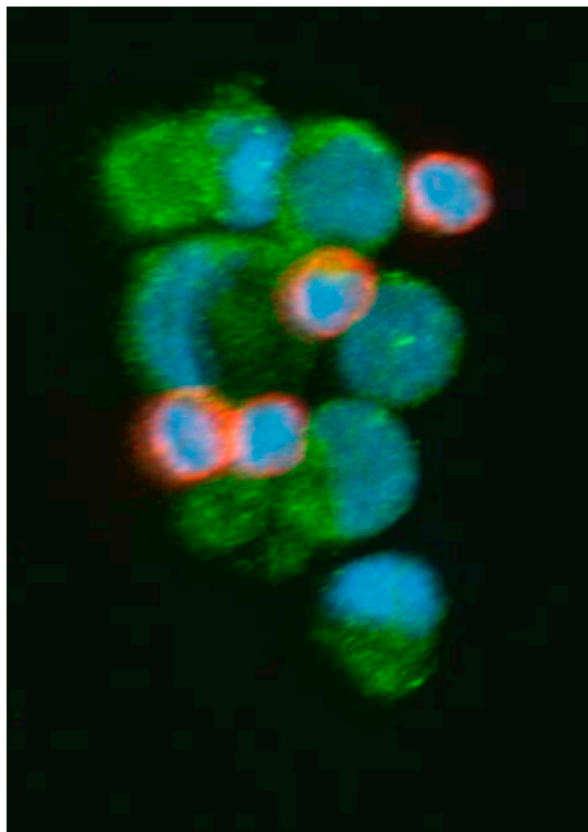
Movie S3. Movie S3 was taken after one cycle of herringbone grooves.

[Movie S3\(MPG\)](#)



Movie S4. Movie S4 shows the flow profiles at the exit of the herringbone device. Corresponding orthogonal projections are shown in Fig. S2.

[Movie S4 \(MPG\)](#)



Movie S5. Rotating confocal image of CTC cluster isolated from a metastatic prostate cancer patient using the HB-Chip.

[Movie S5 \(MPG\)](#)

Table S1. Clinical characteristics and PSA positive, CD45 negative CTC counts for all patients with metastatic prostate cancer presented in Fig. 3A

Patient ID	Gleason sum	PSA+/CD45- CTC/mL	Serum PSA at time of capture	Disease state at time of capture
1	8	75.9	1.84	castration resistant, androgen independent, docetaxel refractory
2	7	14.6	133.80	castration resistant, androgen independent, docetaxel refractory
3	8	0.6	27.61	castration resistant, androgen independent, docetaxel refractory, on clinical trial
4	7	11.5	0.81	castration sensitive
5	7	14.6	133.80	castration resistant, androgen independent, docetaxel refractory
6	8	83.5	4.52	castration sensitive
7	7	18.8	38.21	treatment naïve
8	9	3167.6	8.64	castration resistant, on secondary hormone therapy
9	9	33.4	0.63	castration sensitive
10	9	71.8	0.1	castration sensitive
11	7	235.9	1.49	treatment naïve
12	7	62.7	0.76	castration sensitive
13	N/A	24.0	15.4	castration resistant
14	N/A	63.4	0.38	castration sensitive
15	7	18.2	405.8	castration resistant, androgen independent, docetaxel refractory
16	N/A	1535.5	22.28	treatment naïve

CTC counts for the first HB-Chip stained with the PSA antibody and corresponding clinical characteristics. Evaluated parameters include Gleason sum and serum PSA at the time of CTC analysis.